

# 4

---

## *Photocatalytic Application of Titania Nanoparticles for Degradation of Organic Pollutants*

---

**Hamed Eskandarloo, Alireza Badiei**

School of Chemistry, College of Science, University of Tehran, Tehran, Iran

### **Outline**

Introduction.....	109
Titania nanoparticles .....	111
Synthesis of titania nanoparticles .....	112
Photocatalytic activity of titania nanoparticles .....	115
Doping titania nanoparticles with metallic species .....	115
Coupling titania nanoparticles by other metal oxides .....	118
Effect of additives on photocatalytic efficiency of titania nanoparticles .....	123
Conclusion .....	128
Acknowledgement .....	128
References.....	128

## Introduction

Water is of major importance to all living organisms and generally, accounts almost 70~90 % of their body weight. There is no possible living world without water. Thus, the quality of water resources will directly affect the ordinary life of a human being. The world's population and industry grow have intensified the demand for water supply [1,2]. The chemical contamination of drinking water and aquatic environment has been a serious problem of these last years. Industrial activity consumes large amounts of water and chemicals and produce large amounts of wastewater [3]. The principle sources of industrial wastewaters are dye pollutants [4]. Dye molecules are extensively used in textile dyeing, paper printing, leather, pharmaceutical, cosmetic, and nutrition industries [5]. The textile industry ranks first in usage of dye for coloration of fiber. It is reported that in textile industry, due to inefficiency in the dyeing process, 10~20% of dyes are lost to wastewater. In addition, non-fixed dyes, wastewaters generated by textile industries contain considerable amounts of inorganic salts [6,7].

The removal of industrial wastes from the water has received considerable attention in environmental research. The most often used methods for the treatment of the industrial wastewaters, including membrane filtration, chemical coagulation/flocculation, ion exchange, precipitation, adsorption, biological degradation, and ozonation are not efficient enough and have limitations [8,9].

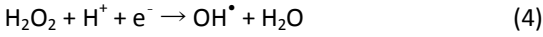
In recent years, a substitute for non-destructive methods is advanced oxidation processes (AOPs), as a most promising way for degradation of various pollutants. The AOPs based on the generation of highly reactive species such as hydroxyl radicals as oxidizing agents that quickly and non-selectively oxidizes a wide range of organic pollutants [10,11]. The AOPs including ultraviolet(UV)/H<sub>2</sub>O<sub>2</sub>, Fenton, photo-Fenton, and heterogeneous photocatalysis, although the use of different reacting systems, the reactive species in all of them are hydroxyl radicals [12,13]. These radicals are very powerful oxidant agents ( $E_0 = 2.8 \text{ V}$ ), which can be used to degrade most organic molecules with rate constants usually in the range of  $10^6$ – $10^9 \text{ M}^{-1} \text{ s}^{-1}$  [14]. If the advanced oxidation operation is carried out under suitable conditions, the final products will be CO<sub>2</sub>, H<sub>2</sub>O, and aliphatic acids with low molecular weight [15].

Heterogeneous photocatalysis technology is an interesting route among AOPs, which can be conveniently used for the complete degradation of various hazardous compounds. Heterogeneous photocatalysis involves a combination of UV or visible light irradiation and an oxide semiconductor (such as TiO<sub>2</sub>, ZnO, ZnS, Fe<sub>2</sub>O<sub>3</sub>, CdS, WO<sub>3</sub>, ZrO<sub>2</sub>, SrO<sub>2</sub>, CeO<sub>2</sub>, etc.) [16,17]. When a semiconductor absorbs a photon with energy greater than or equal to the band gap energy, electrons are promoted from the valence band (VB) to the conduction band (CB) to produce electron-hole pairs, according to Eq. (1): [18]. Schematic of heterogeneous photocatalysis mechanism are shown in Figure 4.1.

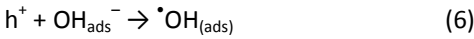
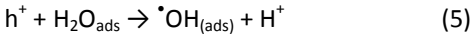


As it can be observed from Figure 4.1, the produced electron-hole pairs can either recombine and release heat energy or interact separately with other molecules [19]. The electrons in the conduction band can reduce dissolved oxygen to superoxide radical anion (Eq. (2)) that this radical may form hydrogen peroxide (Eq. (3)). The electron reduction of hydrogen peroxide produces hydroxyl radical (Eq. (4)) [20].





The holes in the valence band can oxidize the adsorbed water or hydroxide ions to produce hydroxyl radicals (Eqs. (5) and (6)) [21].



Produced free radicals are able to undergo secondary reactions. Among them the hydroxyl radicals can be used to degrade organic compounds at or near these surfaces of semiconductor catalyst, and intermediates are formed. These intermediates react with hydroxyl radicals to produce final products (Eq. (7)) [22].

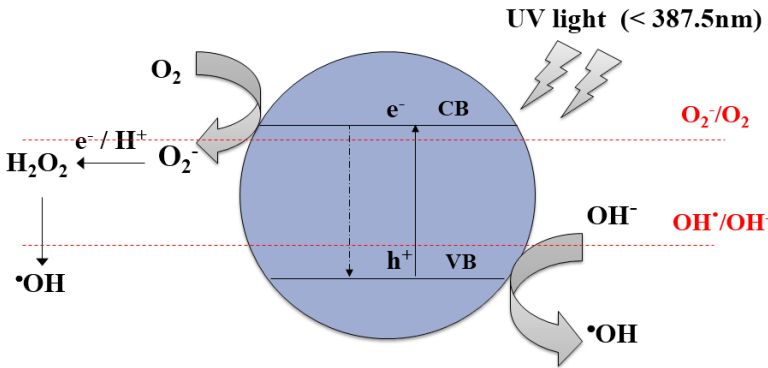


**FIGURE 4.1**

Schematic of heterogeneous photocatalysis mechanism

Generally, two types of photoreactors are used for photocatalytic wastewater treatment processes: (i) slurry photoreactors and (ii) fixed-bed photoreactors. The slurry photoreactors utilize suspended photocatalyst particles, while the other type utilizes immobilized photocatalyst particles on a surface [23]. Nowadays, in most photocatalytic wastewater treatment studies, the catalysts are applied in the form of a slurry. However, the separation of catalyst after the reaction in the slurry systems, is a costly step, which adds to the overall running costs of the plant. Therefore, for practical application of catalysts, immobilized catalyst systems are preferred in order to prevent a costly separation step [24]. However, the immobilized catalyst systems have low interfacial surface areas and consequently a very low activity, and the problem that they are difficult to scale [25]. It is noted that, configuration of photoreactor has an important role in the efficiency of the photocatalytic wastewater treatment processes.

## Titania nanoparticles

Titania ( $\text{TiO}_2$ ) exists in three crystalline phases; anatase, rutile, and brookite. The predominant commercial phase of  $\text{TiO}_2$  is anatase, which has been widely used in photocatalysis processes due to its high photocatalytic activity. Anatase phase has a tetragonal crystal structure and a band gap of 3.23 eV [26,27]. Among the  $\text{TiO}_2$  crystalline phases, rutile is thermodynamically most stable phase than others. Rutile phase has a band gap of 3.0 eV and a crystal structure similar to that of anatase, except that the octahedral shares four edges instead of the four corners [27,28]. Whereas, brookite phase of  $\text{TiO}_2$  has an orthorhombic crystal structure [26,27]. Crystalline structures of  $\text{TiO}_2$  phases are shown in Figure 4.2.

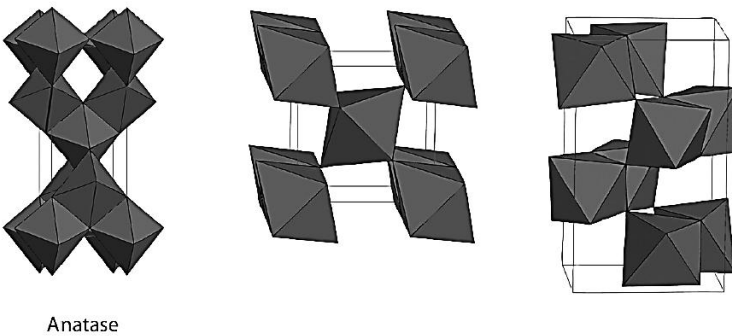
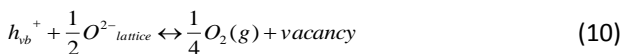


**FIGURE 4.2**  
Crystalline structures of  $\text{TiO}_2$

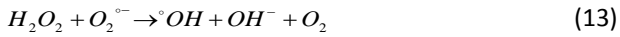
$\text{TiO}_2$  has attracted considerable attention and most of photocatalysis studies have been published on the use of  $\text{TiO}_2$ , as a suitable photocatalyst for the chemical treatment of organic pollutants. The interest in  $\text{TiO}_2$  was mainly due to its availability, low cost, non-toxicity, chemical stability, high photocatalytic activity, and optical–electronic properties [29]. There were some researches on the photocatalysis mechanism of  $\text{TiO}_2$ . A possible mechanism for the photocatalysis mechanism of  $\text{TiO}_2$  indicated that photo-produced electron–hole pairs are trapped at different defect sites. Electron paramagnetic resonance (EPR) results indicate that electrons were trapped as Ti(III) centers (surface-trapped CB electron) and holes were trapped as oxygen-centered radicals covalently linked to the surface of Ti atoms (surface-bound hydroxyl radicals), as shown in Eqs. (8–9) [30,31]:



Also, O vacancies can be formed through the following reaction (Eq. (10)):



Dissolved oxygen is another source of hydroxyl radicals according to the following reactions (Eqs. (11–14)) [31,32]:



Generally, substrate oxidation may occur in three ways: (1) indirect oxidation through the free hydroxyl radicals in solution (2) and/or through the surface-bound hydroxyl radical, and (3) direct oxidation through the valence band holes before it is trapped either at the particle surface or within the particle [33].

## Synthesis of titania nanoparticles

Many techniques are used for the synthesis of TiO<sub>2</sub> nanoparticles (Figure 4.3). Among these techniques, the sol-gel process was currently recognized as one of the most important chemical technique for the synthesis of TiO<sub>2</sub> nanoparticles, due to several advantages, such as low processing temperature, versatility of processing, high homogeneity, and stability [34,35].

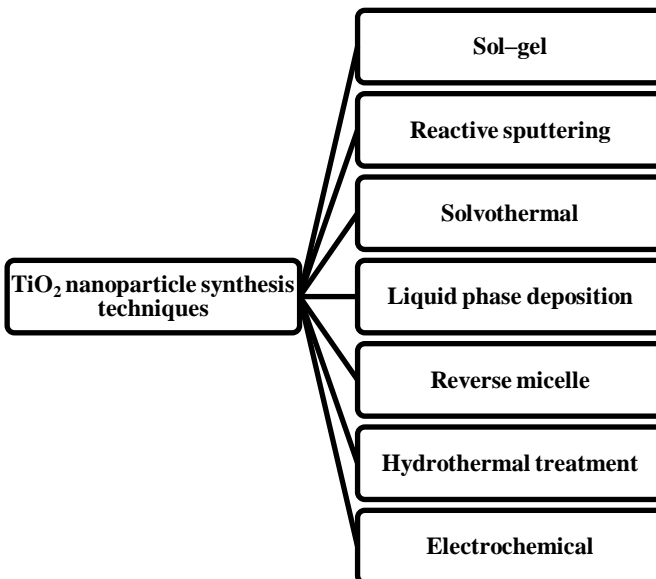


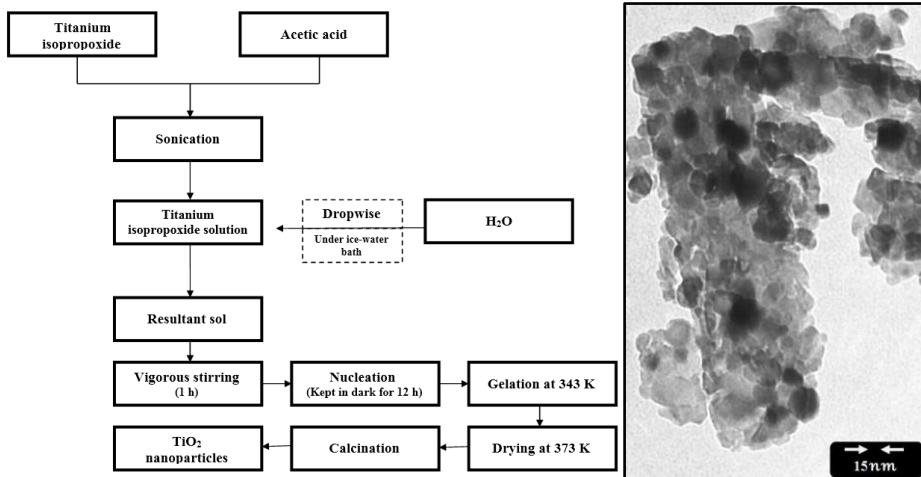
**FIGURE 4.3**

Synthesis techniques of TiO<sub>2</sub> nanoparticles

Some reports on the sol-gel preparation of TiO<sub>2</sub> nanoparticles will be reviewed here: Bessekhoud et al. [36] employed the sol-gel process for the synthesis of nanostructured TiO<sub>2</sub> from the metal alkoxide precursor (titanium tetraisopropoxide, Ti(OC<sub>3</sub>H<sub>7</sub>)<sub>4</sub>) and a mixture of two alcohols (methanol and ethanol) as solvent. For this purpose, metal alkoxide precursor was dissolved in a

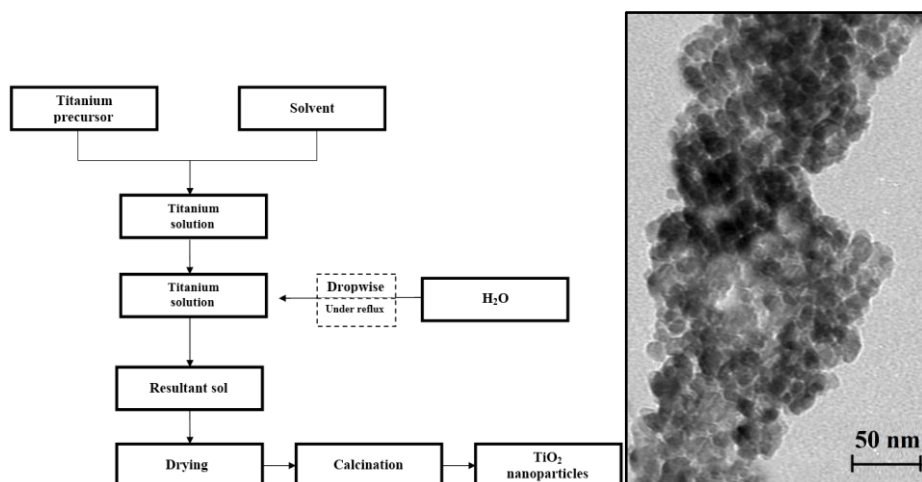
mixture of methanol and ethanol. Then water was added dropwise into the above solution under reflux. The obtained precipitate was filtered and washed with hot water and organic solvents to remove the adsorbed impurities. Then heated at 110 °C for 12 h. They studied the effect of synthesis variables, such as the amount of water and solvent, reflux time, and temperature on photocatalytic activity of prepared TiO<sub>2</sub> nanoparticles in the removal of Malachite Green as a model pollutant. The optimum conditions for the synthesis of TiO<sub>2</sub> nanoparticles with high photocatalytic activity were as follows; 1:1:75 for precursor/solvent/water molar ratios, 75 °C reflux temperature, and 3 h reflux time. They have concluded that the number of active sites can depend on the water amount. In the presence of higher amounts of water, high hydrolysis rates are desired for the formation of Ti(OH)<sub>4</sub>, which condense to yield Ti–O–Ti chains. The hydrolysis of metal alkoxide precursor produces Ti–OH, which can react with an alkoxide molecule or another Ti–OH species or a solvated metal species. The ratio of water to metal alkoxide precursor determines the contribution of each reaction and consequently, the mechanism of the reaction. The excess water suppresses the development of Ti–O–Ti species, because chemical equilibrium causes the favorable creation of Ti–OH species.

In another study, Behnajady and Eskandarloo [37–39] employed the sol–gel low temperature and sol–gel high temperature methods for synthesis of anatase–type and mixed anatase/rutile–type TiO<sub>2</sub> nanoparticles, respectively. In sol–gel low temperature synthesis, titanium tetraisopropoxide was used as a precursor and glacial acetic acid used as a chelating agent for control the hydrolysis of titania precursor and efficient stabilizer of the anatase phase. The schematic of the sol–gel low temperature is shown in Figure 4.4a. The effects of synthesis parameters such as acetic acid and water ratios, sol formation time, and calcination temperature on the structural and photocatalytic activity of anatase–type TiO<sub>2</sub> nanoparticles were investigated. They have concluded that the acetic acid inhibits the rapid hydrolysis of titania precursor and resulting in control produces of Ti–OH species. During condensation, two Ti–OH species can link together to form Ti–O–Ti species. Then polymerization process produces polynuclear complex of Ti–O–Ti species which will precipitate in the result of their large size. Therefore, the Ti–O–Ti species in high acidic media possesses a higher polymerization rate and resulting in the larger crystalline sizes of the TiO<sub>2</sub> nanoparticles. The mean size of prepared anatase–type TiO<sub>2</sub> particles is estimated to be less than 15 nm from transmission electron microscopy (TEM) image (Figure 4.4b). In order to study the effect of calcination temperature on anatase phase stability, prepared nanoparticles was calcined at different temperatures from 450 to 750 °C for 3 h. The XRD patterns reveal that calcined samples below than 650 °C had completely anatase structure and calcined sample at 750°C was a combination of anatase/rutile phases. It was interesting to observe that with increasing calcination temperature to 750 °C, only some portion of anatase phase transformed to rutile phase, whereas other studies had shown reported temperature of 600–650°C for complete transformation of anatase to rutile phase. They have concluded that the sol–gel low temperature method is able to synthesis TiO<sub>2</sub> nanoparticles with stable anatase structure. The photocatalytic activity of prepared TiO<sub>2</sub> nanoparticles was evaluated in the removal of C.I. Acid Red 27 as a model contaminant from textile industry. The optimum conditions for low temperature synthesis of anatase–type TiO<sub>2</sub> nanoparticles with high photocatalytic activity were as follows; 1:1:200 for titanium precursor/acetic acid/water molar ratios, 1 h sol formation time, 0 °C synthesis temperature, and 450 °C calcination temperature.

**FIGURE 4.4**

(a) Scheme of the sol-gel low temperature synthesis method and (b) TEM image of the prepared anatase-type TiO<sub>2</sub> nanoparticles

In sol-gel high temperature method for synthesis of mixed anatase/rutile-type TiO<sub>2</sub> nanoparticles, the effect of synthesis variables, including precursor and solvent type, reflux temperature and time, solvent and water molar percent, gelation pH, sol drying method, and calcination temperature were studied. In this method, various precursors such as titanium tetraisopropoxide and titanium n-butoxide and various solvents such as methanol, ethanol, and isopropanol used as solvent. The hydrolysis process was performed by adding of drop by drop water into a flask containing precursor/solvent mixture under reflux and magnetic stirring. The schematic of the sol-gel high temperature method and TEM image of prepared mixed anatase/rutile-type TiO<sub>2</sub> nanoparticles are shown in Figure 4.5. Structural characterizations and photocatalytic activity evaluations have proved that the structure and photocatalytic activity of prepared TiO<sub>2</sub> nanoparticles are functions of precursor type, solvent type, and other synthesis conditions. The optimum conditions for high temperature synthesis of mixed phase anatase-rutile TiO<sub>2</sub> nanoparticles with high photocatalytic activity were as follows: titanium (IV) isopropoxide as precursor, methanol as solvent, 3 h reflux time, 80 °C reflux temperature, gelation pH of 5, thermal drying of sol, and 450 °C calcination temperature. Behnajady and Eskandarloo studies clearly revealed that the sol-gel synthesis variables affect the structural properties of TiO<sub>2</sub> catalyst such as the particle size, phase composition, band gap, pore volume, surface area, and accordingly affect its photocatalytic activity.

**FIGURE 4.5**

(a) Scheme of the sol–gel high temperature synthesis method and (b) TEM image of the prepared mixed phase anatase–rutile TiO<sub>2</sub> nanoparticles

## Photocatalytic activity of titania nanoparticles

The rate of photocatalytic activity of TiO<sub>2</sub> catalyst is limited to the recombination rate of photo-produced electron–hole pairs. The quick recombination of photo-induced charge carriers decreases the photocatalytic efficiency of TiO<sub>2</sub> catalyst [40,41]. In order to reduce electron–hole recombination and improve the photocatalytic activity of TiO<sub>2</sub>, some of techniques have been used, including doping by various metallic species and coupling with other semiconductors [42–44].

### *Doping titania nanoparticles with metallic species*

Doping of TiO<sub>2</sub> with various metallic species is one possible solving route to prevent the recombination of charge carriers. The metal nanoparticles on the surface of TiO<sub>2</sub> will act as an electron reservoir to trap electrons which can greatly increase the efficiency of charge separation, resulting in the improvement of TiO<sub>2</sub> photocatalytic activity. Furthermore, the addition of dopants can change the surface properties of TiO<sub>2</sub> catalyst such as surface area and surface acidity [45]. Some reports on the doping of TiO<sub>2</sub> nanoparticles will be reviewed here: Castro et al. [46] prepared doped anatase–structure TiO<sub>2</sub> nanoparticles (Sb/TiO<sub>2</sub>, Nb/TiO<sub>2</sub>, Fe/TiO<sub>2</sub>, and Co/TiO<sub>2</sub>) by means of a hydrothermal methodology preceded by a precipitation doping step. TEM images of Fe:TiO<sub>2</sub> and Sb/TiO<sub>2</sub> nanoparticles, showed a morphology similar to that the un-doped pure TiO<sub>2</sub> sample, whereas, Nb/TiO<sub>2</sub> and Co/TiO<sub>2</sub> nanoparticle, showed particles with an elongated morphology (Figure 4.6). The photocatalytic activity of the doped anatase–structure TiO<sub>2</sub> nanoparticles was examined in degradation of diquat dibromide monohydrate as a model compound. The results revealed a significant enhancement in the photocatalytic activity of the Sb/TiO<sub>2</sub> and Nb/TiO<sub>2</sub> nanoparticles, whereas no photocatalytic activity was detected for the Fe/TiO<sub>2</sub> and Co/TiO<sub>2</sub> nanoparticles. By using Mossbauer spectroscopy and magnetization data, the obtained results were correlated to the doping ions oxidation states. They have concluded that both amount and valence

of the doping ions are important factors that strongly determine the photocatalytic activity of doped  $\text{TiO}_2$  nanoparticles.

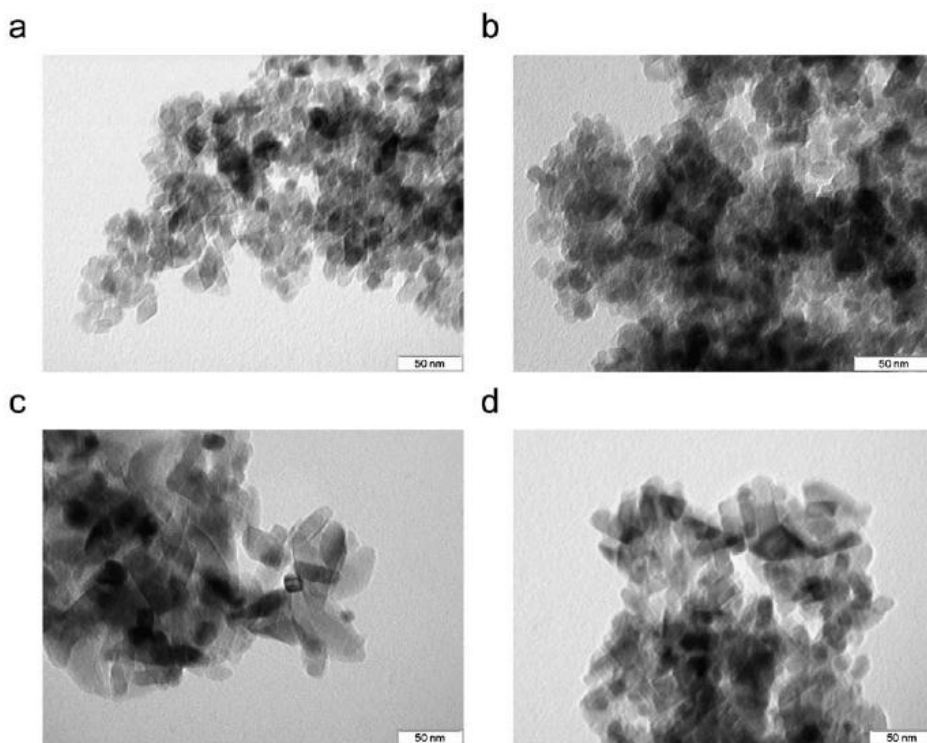
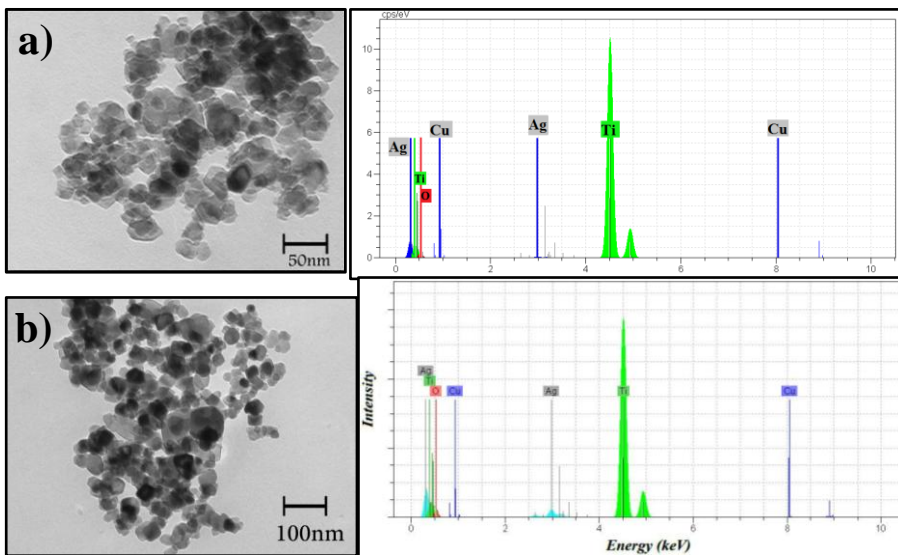


**FIGURE 4.6**

TEM images of doped  $\text{TiO}_2$  nanoparticles: (a)  $\text{Fe}:\text{TiO}_2$ , (b)  $\text{Sb}:\text{TiO}_2$ , (c)  $\text{Nb}:\text{TiO}_2$ , and (d)  $\text{Co}:\text{TiO}_2$

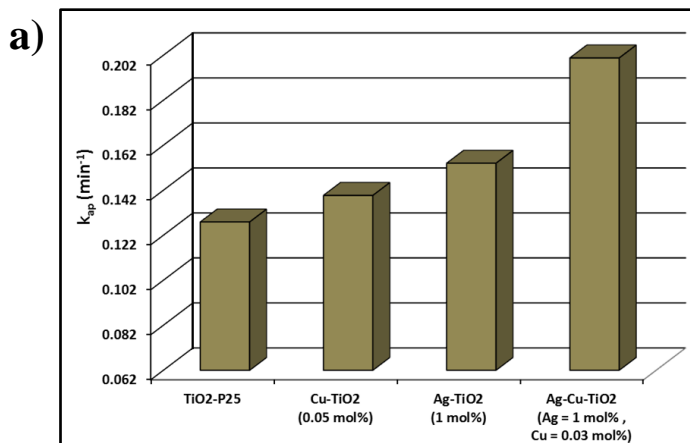
However,  $\text{TiO}_2$  doped by a single species has not been found to meet practical applications and reported that co-doping with different species leads to higher photocatalytic activity. Behnajady and Eskandarloo [17,47] used sol-gel prepared  $\text{TiO}_2$  nanoparticles and commercially available  $\text{TiO}_2$ -P25 nanoparticles for direct and indirect doping of silver and copper. From TEM images of co-doped  $\text{Ag,Cu}/\text{TiO}_2$  nanoparticles (Figure 4.7(a–b)), a mean size of 10–35 nm and 20–30 nm is estimated for direct and indirect co-doped samples, respectively. Energy-dispersive X-ray spectroscopy (EDX) analysis at the microscopic level confirmed the presence of both silver and copper metals in chemical composition of the direct and indirect co-doped samples (Figure 4.7(a–b)). The photocatalytic activity of prepared nanoparticles was evaluated in the removal of C.I. Acid Orange 7 as a model pollutant from textile industry. In both direct and indirect doping methods, co-doped  $\text{Ag,Cu}/\text{TiO}_2$  nanoparticles showed the highest photocatalytic activity compared to mono-doped  $\text{Ag}/\text{TiO}_2$ ,  $\text{Cu}/\text{TiO}_2$ , and pure  $\text{TiO}_2$  nanoparticles under both UV and visible light irradiation. Comparison between the photocatalytic activity of  $\text{TiO}_2$ ,  $\text{Cu}/\text{TiO}_2$ ,  $\text{Ag}/\text{TiO}_2$ , and  $\text{Ag,Cu}/\text{TiO}_2$  nanoparticles prepared by the indirect doping method is shown in Figure 4.8. The optimum contents of silver and copper dopant ions were (0.08 mol% Ag/0.01 mol% Cu) and (0.1 mol% Ag/0.03 mol% Cu), for direct and indirect co-doped samples, respectively. The positive effect of Ag on the photocatalytic activity of  $\text{TiO}_2$  nanoparticles was explained by Ag ability to trap electrons and

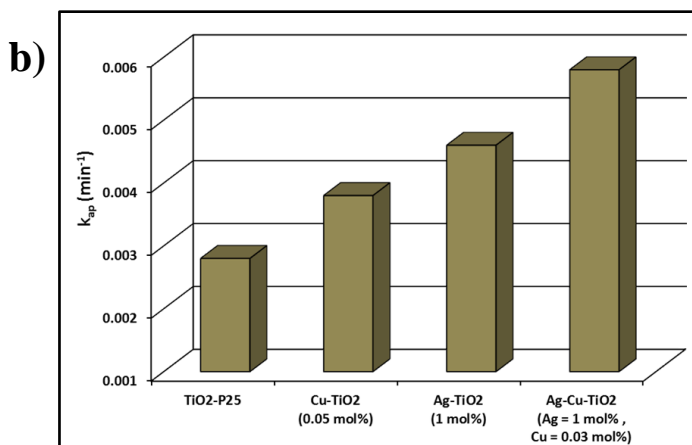
its ability to modify the interfacial charge transfer to electron acceptors. Due to the Fermi level of Ag is lower than that of  $\text{TiO}_2$  conduction band and the formation of Schottky barrier in the  $\text{TiO}_2$  and Ag contact region, electrons in the conduction band of  $\text{TiO}_2$  catalyst transfer to Ag metal. The electrons transferred to the Ag cluster react with adsorbed  $\text{O}_2$  molecules and form superoxide anions. On the other hand, the holes will be free and react with adsorbed water and hydroxide ions to form hydroxyl radicals. Therefore, this process prevents the recombination of photo-produced electron-hole pairs and will be useful for significant enhancement in the photocatalytic activity of the  $\text{TiO}_2$  nanoparticles. In addition, in the case of the positive effect of Cu on the photocatalytic activity of  $\text{TiO}_2$  nanoparticles, due to the reduction potential of CuO is greater than that of  $\text{TiO}_2$ , CuO by capturing of photo-produced electrons reduce to  $\text{Cu}_2\text{O}$  or Cu, and resulting in inhibits the recombination of electron-hole pairs and enhancement in the photocatalytic activity.



**FIGURE 4.7**

TEM images and EDX spectrum of Ag,Cu/ $\text{TiO}_2$  nanoparticles prepared by (a) direct and (b) indirect doping methods

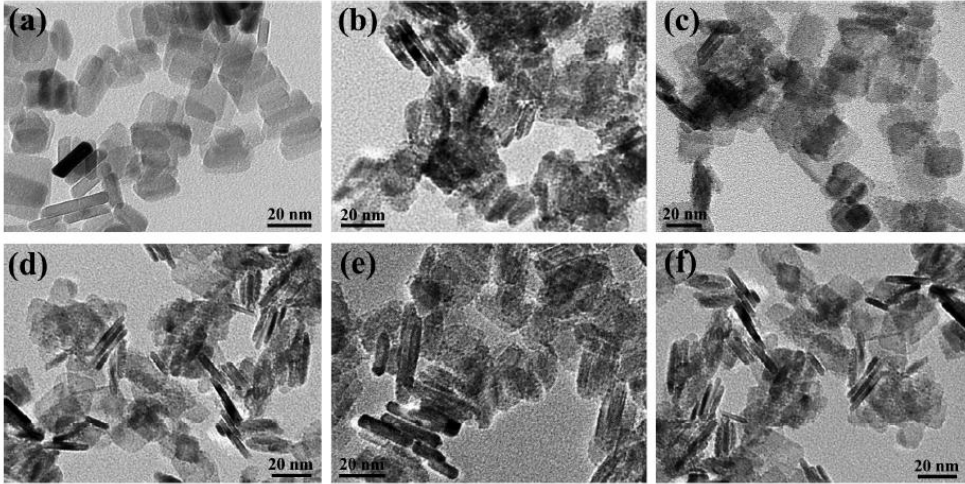


**FIGURE 4.8**

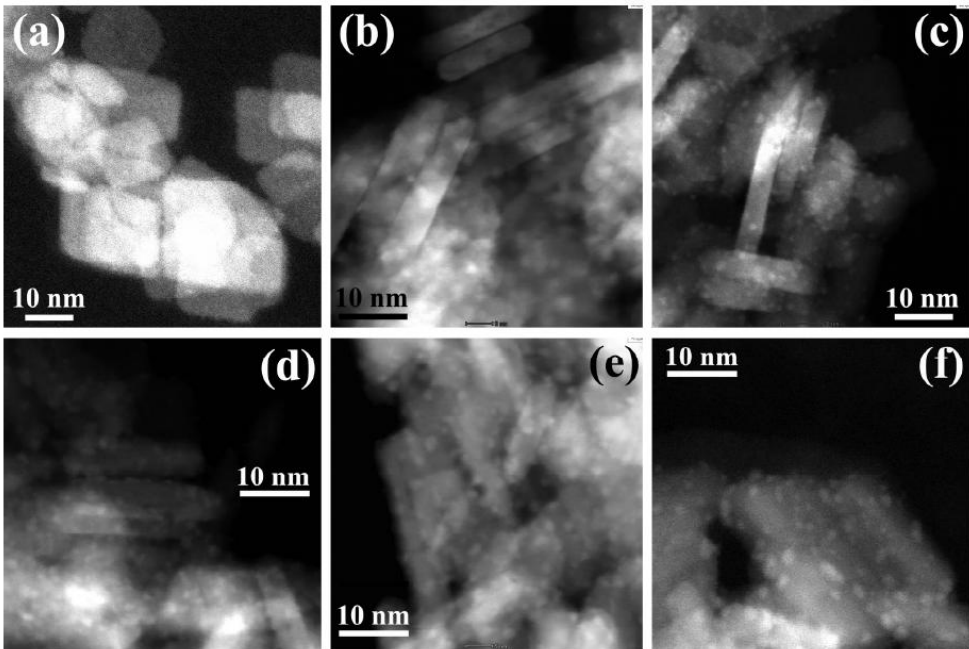
Comparison between the photocatalytic activity of TiO<sub>2</sub>, Cu/TiO<sub>2</sub>, Ag/TiO<sub>2</sub>, and Ag,Cu/TiO<sub>2</sub> nanoparticles prepared by the indirect doping method in the removal of AO7 under (a) UV and (b) visible light irradiation

### ***Coupling titania nanoparticles by other metal oxides***

TiO<sub>2</sub> coupling with other metal oxides is another approach in order to increase the lifetime of the photo-produced electron-hole pairs and improve the photocatalytic activity of TiO<sub>2</sub>. Recently, many studies related to TiO<sub>2</sub> coupled with other metal oxides, such as ZnO-TiO<sub>2</sub>, ZrO<sub>2</sub>-TiO<sub>2</sub>, SnO<sub>2</sub>-TiO<sub>2</sub>, Cu<sub>2</sub>O-TiO<sub>2</sub>, WO<sub>3</sub>-TiO<sub>2</sub>, and CeO<sub>2</sub>-TiO<sub>2</sub>, have been reported [48]. Some reports on the coupling of TiO<sub>2</sub> nanoparticles will be reviewed here; Liu et al. [49] have reported one-pot preparation of transition metal oxide clusters (MnO<sub>x</sub>, FeO<sub>x</sub>, CoO<sub>x</sub>, NiO<sub>x</sub>, and CuO<sub>x</sub>) loaded on TiO<sub>2</sub> nanosheets. By using TEM and scanning transmission electron microscopy (STEM) techniques, Figure 4.9 and 4.10, they have concluded that the metal oxide do not dope into the frameworks of TiO<sub>2</sub> nanosheets, rather the metal oxide clusters with ~2 nm size were dispersed on TiO<sub>2</sub> nanosheets. The metal oxide clusters loaded TiO<sub>2</sub> samples show similar morphology compared with pure TiO<sub>2</sub>, indicating that the addition of other metal oxide not impact the growth of TiO<sub>2</sub> nanosheets. From photoluminescence (PL) and photoelectrochemical measurements, they have suggested that these metal oxide clusters can capture photo-produced hole and consequently leading to higher electron-hole separation efficiency. Because the heterojunctions are formed between TiO<sub>2</sub> nanosheets and the metal oxide clusters, favoring charge transfer across the interface. Photocatalytic O<sub>2</sub> evolution from water oxidation under UV light was used to test the photocatalytic activity of prepared samples. Metal oxide clusters loaded TiO<sub>2</sub> nanosheets, especially MnO<sub>x</sub>/TiO<sub>2</sub> and CoO<sub>x</sub>/TiO<sub>2</sub>, showed significant photocatalytic water oxidation to O<sub>2</sub> compared to pure TiO<sub>2</sub> nanosheets. Because of their advantages in fast interface charge transfer and highly active holes, MnO<sub>x</sub>/TiO<sub>2</sub> and CoO<sub>x</sub>/TiO<sub>2</sub> show excellent photocatalytic performance in water oxidation. They have concluded, that the transition metal oxide clusters on TiO<sub>2</sub> nanosheets can also serve as co-catalysts and participate in photocatalysis process.

**FIGURE 4.9**

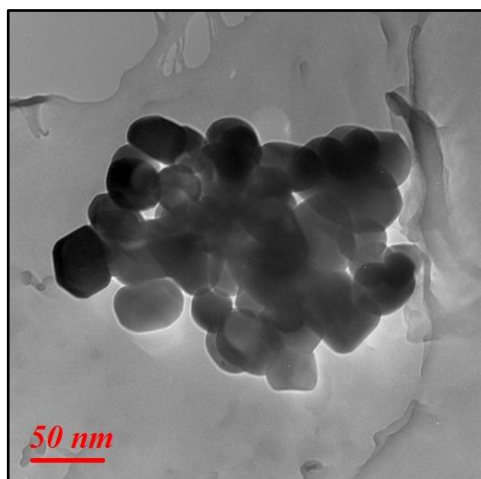
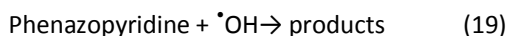
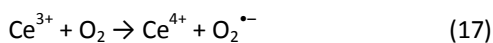
TEM images of (a) pure TiO<sub>2</sub>, (b) Mn-TiO<sub>2</sub>, (c) Fe-TiO<sub>2</sub>, (d) Co-TiO<sub>2</sub>, (e) Ni-TiO<sub>2</sub>, and (f) Cu-TiO<sub>2</sub> nanosheets

**FIGURE 4.10**

STEM images of (a) pure TiO<sub>2</sub>, (b) Mn-TiO<sub>2</sub>, (c) Fe-TiO<sub>2</sub>, (d) Co-TiO<sub>2</sub>, (e) Ni-TiO<sub>2</sub>, and (f) Cu-TiO<sub>2</sub> nanosheets

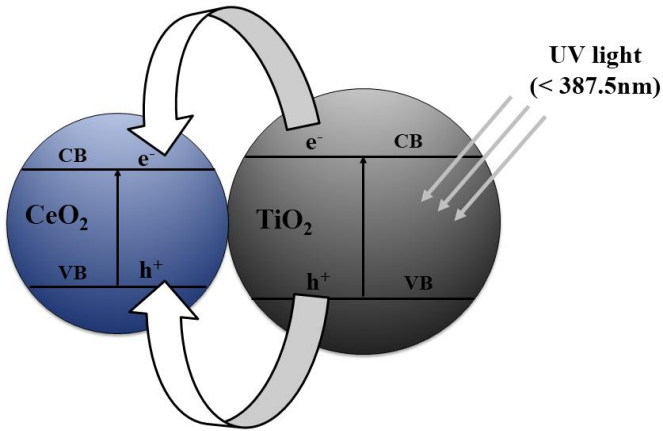
Eskadnarloo et al. [50] prepared TiO<sub>2</sub>/CeO<sub>2</sub> coupled nanoparticles and used them in the photocatalytic removal of phenazopyridine as a model drug contaminant under UV light irradiation. They employed response surface methodology (RSM) to optimize the individual and interactional effects of the synthesis variables. Their study results indicated that the maximum removal

efficiency was achieved at the optimum synthesis conditions: Ti/Ce weight ratio of 0.84:0.16, calcination temperature of 502 °C, and calcination time of 62 min. The TEM image of the optimized TiO<sub>2</sub>/CeO<sub>2</sub> coupled nanoparticles showed that the mean particle size is about 30–40 nm (Figure 4.11). A comparison of single and coupled photocatalysts for photocatalytic removal of the phenazopyridine has been performed. The results showed that the highest removal efficiency (66.64%) was obtained using TiO<sub>2</sub>/CeO<sub>2</sub> coupled nanoparticles, whereas at the same time, using TiO<sub>2</sub> and CeO<sub>2</sub> samples lead to 55.63% and 19.1% removal efficiency, respectively. They have suggested that the coupling TiO<sub>2</sub> with CeO<sub>2</sub> could produce special electrons and holes transfer from TiO<sub>2</sub> to CeO<sub>2</sub>, which is able to facilitate the separation of the electron–hole pairs and thus improve the photocatalytic activity of the coupled photocatalyst. They justify their results by a simple mechanism representation of the coupled CeO<sub>2</sub>/TiO<sub>2</sub> that is responsible for its UV light activity (Figure 4.12). From diffuse reflectance spectroscopy (DRS) results, they reported that the energy band gap of TiO<sub>2</sub> (3.26 eV) is bigger than that of CeO<sub>2</sub> (2.01 eV), therefore, the energy level of the conduction band of TiO<sub>2</sub> is higher than the corresponding ones of CeO<sub>2</sub>, which this feature can cause the electron transfer from TiO<sub>2</sub> to CeO<sub>2</sub>. On the other hand, the energy level of the valence band of CeO<sub>2</sub> is higher than the corresponding one of TiO<sub>2</sub>, which this feature can cause transferring of the holes from TiO<sub>2</sub> to CeO<sub>2</sub>. Finally, the complete separation of electron–hole pairs in TiO<sub>2</sub> occurs, resulting in the improvement of the photocatalytic activity of the TiO<sub>2</sub> photocatalysts with increasing O<sub>2</sub><sup>•-</sup> and hydroxyl radical generation through the following equations (15–19);



**FIGURE 4.11**

TEM image of the TiO<sub>2</sub>/CeO<sub>2</sub> coupled photocatalyst

**FIGURE 4.12**

Possible photocatalytic mechanism of  $\text{TiO}_2/\text{CeO}_2$  coupled nanoparticles under UV light irradiation

In another work, Eskandarloo et al. [51] prepared  $\text{TiO}_2/\text{NiO}$  coupled nanoparticles by using impregnation technique and then were immobilized the prepared nanoparticles on glass plate and used as a fixed-bed photocatalytic system for photodegradation of Acid Fuchsin, as a triphenylmethane dye pollutant. The high-resolution transmission electron microscopy (HRTEM) image of the  $\text{TiO}_2/\text{NiO}$  coupled nanoparticles were directly shown that the small NiO particles (<math>< 10\text{ nm}</math>) dispersed on the surface of  $\text{TiO}_2$  particles ( $\sim 50\text{ nm}$ ) (Figure 4.13). A comparison on photocatalytic activity of immobilized pure  $\text{TiO}_2$  and  $\text{TiO}_2/\text{NiO}$  nanoparticles, showed that the  $\text{TiO}_2/\text{NiO}$  has a higher photocatalytic efficiency than pure  $\text{TiO}_2$  (Figure 4.14). They justify their results by a simple mechanism representation for the photocatalytic activity of  $\text{TiO}_2/\text{NiO}$  under UV light irradiation (Figure 4.15). When  $\text{TiO}_2$  as a n-type electron-rich semiconductor is in contact with NiO as a p-type hole-rich semiconductor, at n-p junction interfacial contact produces a space charge region. The holes are diffused from  $\text{TiO}_2$  to NiO and electrons are diffused from NiO to  $\text{TiO}_2$ . Finally, the complete separation of electron-hole pairs in  $\text{TiO}_2$  occurs, resulting in the improvement of the photocatalytic activity of the  $\text{TiO}_2$  nanoparticles. They have reported that the direct photolysis of Acid Fuchsin solution under UV light irradiation alone had no significant change in the concentration of Acid Fuchsin. Also, the adsorption capability of immobilized  $\text{TiO}_2/\text{NiO}$  nanoparticles was performed in darkness, when the UV lamp had been switched off and the reaction was allowed to continue in the darkness. The results indicate that the dye removal rate was negligible 5.4%. From these experiments they have concluded that both photocatalysts and UV light irradiation were needed for the effective photocatalytic degradation.

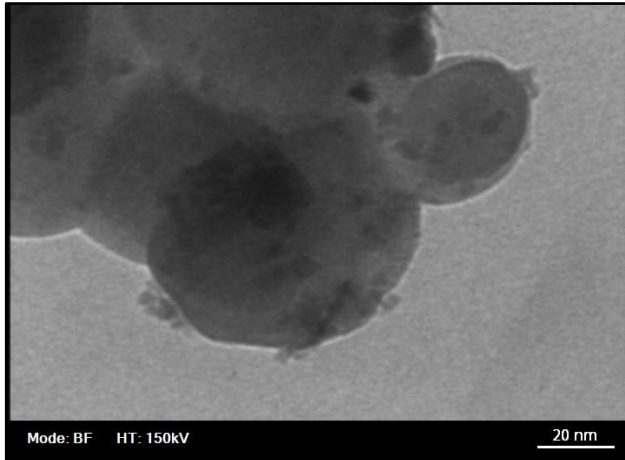


**FIGURE 4.13**  
HRTEM image of  $\text{TiO}_2/\text{NiO}$  nanoparticles

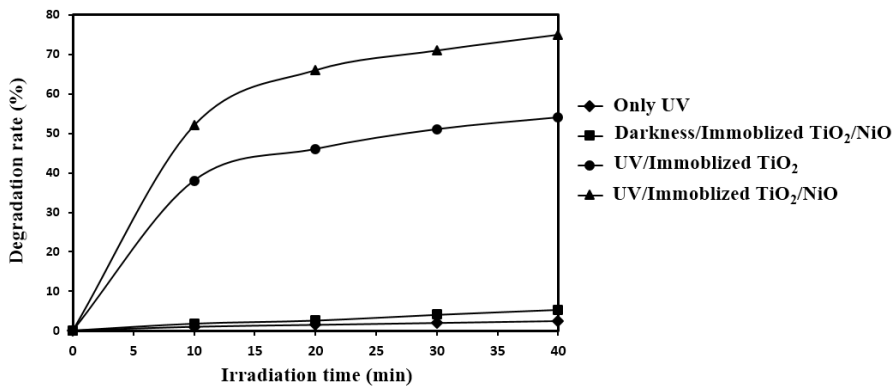


**FIGURE 4.14**  
Direct photolysis, adsorption in the darkness, and photocatalytic degradation of Acid Fuchsin in the presence of immobilized pure  $\text{TiO}_2$  and  $\text{TiO}_2/\text{NiO}$  nanoparticles

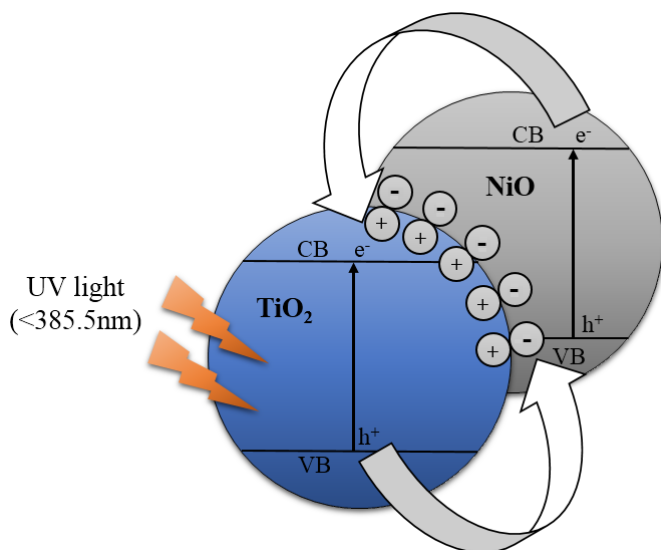


**FIGURE 4.15**

Possible mechanism for photocatalytic activity of  $\text{TiO}_2/\text{NiO}$  coupled nanoparticles

## Effect of Additives on photocatalytic efficiency of titania nanoparticles

Wastewaters usually contain considerable amount of inorganic anions (such as nitrates, carbonates, sulfates, phosphates, etc.) coexisting with organic contaminants. Inorganic anions have an effect on the heterogeneous photocatalytic process, by changing the ionic strength of the reaction medium and inhibiting the catalytic activity of the photocatalyst [52,53]. In addition to the inorganic anions, wastewaters usually contain various dissolved metal ions, which can affect the rate of photocatalytic processes [54].

In heterogeneous photocatalytic processes, oxygen on the catalyst surface acts as an electron acceptor for the prevention of the electron–hole recombination process. When the mass transfer of oxygen in the reaction medium is slow or oxygen is consumed, inorganic oxidants can compensate for the lack of oxygen. In photocatalytic processes, inorganic oxidants increase the electron–hole separation time, by accepting the conduction band electron, which are excited by irradiation of the catalyst, resulting in the improvement of the photocatalytic activity [55,56].

Eskandarloo et al. [51] were investigated the effects of nature and concentration of various additives such as inorganic anions (such as  $\text{CH}_3\text{COO}^-$ ,  $\text{CO}_3^{2-}$ ,  $\text{NO}_3^-$ ,  $\text{Cl}^-$ ,  $\text{H}_2\text{PO}_4^-$ , and  $\text{SO}_4^{2-}$ ), inorganic oxidants (such as  $\text{HSO}_5^-$ ,  $\text{IO}_4^-$ ,  $\text{ClO}_3^-$ ,  $\text{S}_2\text{O}_8^{2-}$ ,  $\text{H}_2\text{O}_2$ , and  $\text{BrO}_3^-$ ), and transition metal ions (such as  $\text{Co}^{2+}$ ,  $\text{Zn}^{2+}$ ,  $\text{Fe}^{2+}$ ,  $\text{Cu}^{2+}$ ,  $\text{Ni}^{2+}$ , and  $\text{Mn}^{2+}$ ) on the photocatalytic efficiency of  $\text{TiO}_2/\text{NiO}$  fixed–bed system. Their results showed that the nature and concentration of additives significantly affected the photocatalytic efficiency of  $\text{TiO}_2/\text{NiO}$  fixed–bed system. The inorganic anions showed a negative effect on the photocatalytic degradation rate of Acid Fuchsin dye, whereas transition metal ions and inorganic oxidants showed a positive effect (Figure 4.16). They reported that the positive effect of inorganic oxidants was in the order of  $\text{IO}_4^- > \text{S}_2\text{O}_8^{2-} > \text{H}_2\text{O}_2 > \text{HSO}_5^- > \text{BrO}_3^- > \text{ClO}_3^-$  and for metal

ions was in the order of  $\text{Cu}^{2+} > \text{Ni}^{2+} > \text{Co}^{2+} > \text{Fe}^{2+} > \text{Zn}^{2+} > \text{Mn}^{2+}$ . Whereas the negative effect of inorganic anions was in the order of  $\text{H}_2\text{PO}_4^- > \text{CO}_3^{2-} > \text{CH}_3\text{COO}^- > \text{Cl}^- > \text{SO}_4^{2-} > \text{NO}_3^-$ .

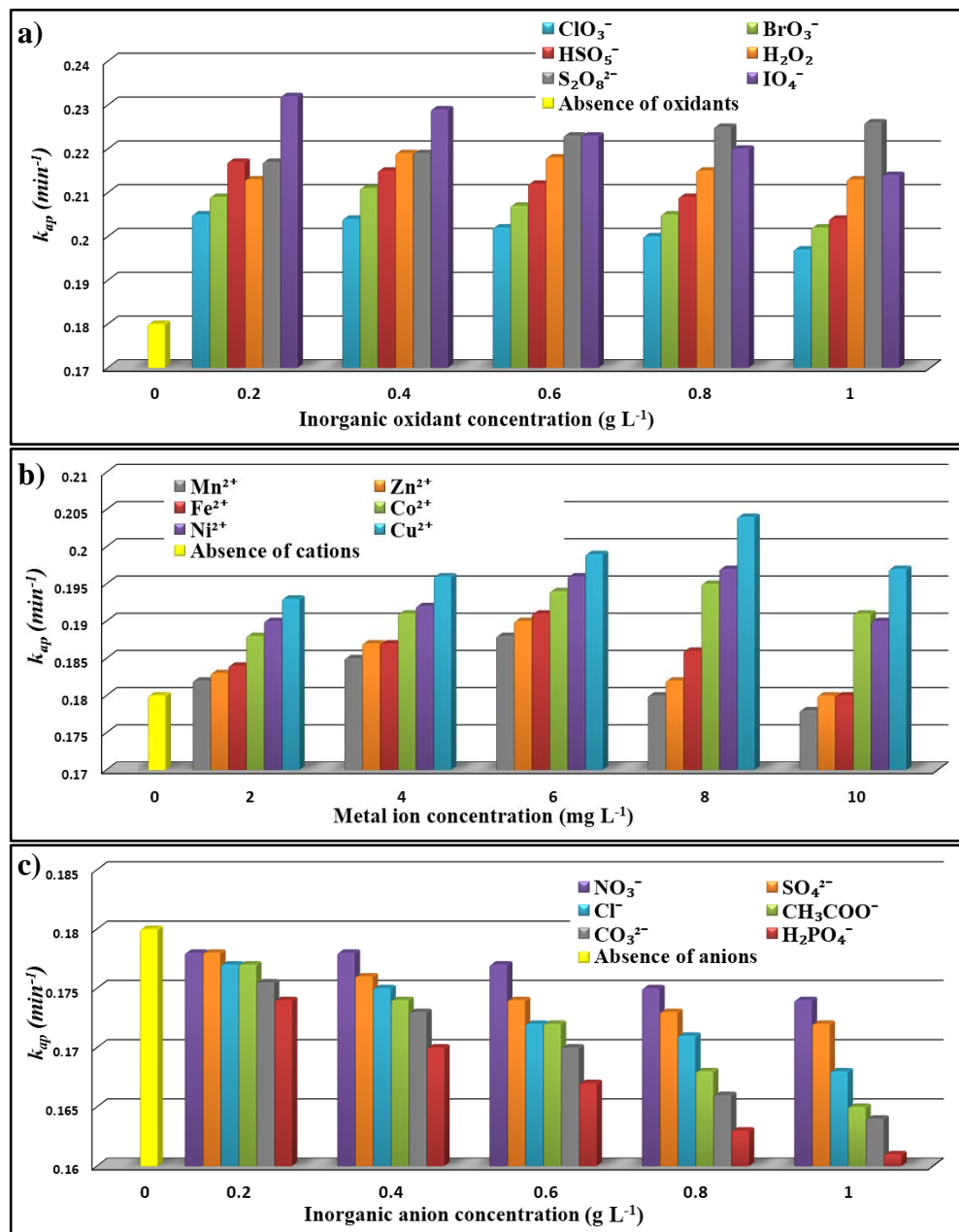


**FIGURE 4.16**

Effects of (a) inorganic oxidants, (b) transition metal ions, and (c) inorganic anions concentration on the photocatalytic degradation rate of Acid Fuchsin dye

The positive effect of transition metal ions was explained by two factors; (i) The surface of TiO<sub>2</sub>/NiO coupled nanoparticles in a fixed-bed system becomes slightly positively charged, when the transition metal ions get adsorbed to the surface. Therefore, the adsorption of Acid Fuchsin molecules effectively occurs on the TiO<sub>2</sub>/NiO surface because Acid Fuchsin molecules are anionic and the catalyst surface as the result of cation adsorption is positively charged. (ii) On the other hand, transition metal ions behave as a scavenger of electron and preventing of electron-hole recombination (Eq. (20)), resulting in the increasing the chances of the  $\cdot\text{OH}$  formation on the TiO<sub>2</sub>/NiO surface.

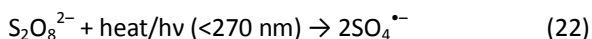


M = Co, Cu, Zn, Fe, Ni, Mn

In study the effects of metal ions concentration on the photocatalytic efficiency of TiO<sub>2</sub>/NiO fixed-bed system, they have concluded that with increasing concentration of dissolved transition metal ions, the photocatalytic degradation of Acid Fuchsin become faster, but further increasing in metal ions concentration in reaction medium leads to a decline in the photocatalytic degradation rate of Acid Fuchsin. The negative effect of high metal ions concentration was explained by this fact which limited the concentration of metal ions, the high metal ions concentration has a filter effect due to UV light absorption and reduces the light intensity in the reaction medium, thus lowering the photocatalytic degradation rate. Also, when the concentration of dissolved transition metal ions is higher, the M<sup>+</sup> ions produced by the electrons and exists as the predominant ions in the reaction medium, that the M<sup>+</sup> ions are oxidized to M<sup>2+</sup> by the photoinduced h<sup>+</sup> on the surface of TiO<sub>2</sub>/NiO catalysts (Eq. (21)).



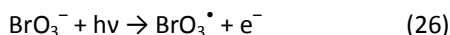
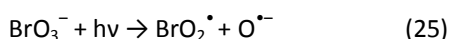
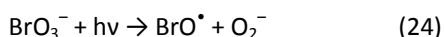
The positive effect of inorganic oxidants on the photocatalytic efficiency of TiO<sub>2</sub>/NiO fixed-bed system was explained with the scavenging of photogenerated electrons by inorganic oxidants (Figure 4.17) and consequently increasing electron-hole separation time. They have reported that the combination of inorganic oxidants and UV radiation provides a strong oxidant system through generation of other oxidizing species, and therefore they play a dual role in photocatalytic process. UV/inorganic oxidants extensively used as an alternative method for removal of various organic pollutants from aqueous solutions. Peroxydisulfate is a thermodynamically strong oxidizing agent (with a redox potential of 2.05 V) that has been used as a sacrificial reagent and alternative oxidant in the chemical oxidation of organic contaminants. Undergo photolysis or thermolysis in aqueous solution, S<sub>2</sub>O<sub>8</sub><sup>2-</sup> decomposes to generate the free sulfate (SO<sub>4</sub><sup>•-</sup>) oxidant (Eq. (22)). SO<sub>4</sub><sup>•-</sup> as a very strong oxidizing agent (with a redox potential of 2.6 V) can accelerate the reaction through producing a rapid attack to any oxidizable agent [57–59].



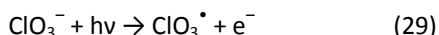
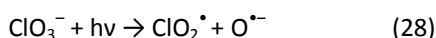
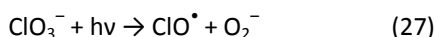
Peroxymonosulfate is an inexpensive and effective acidic oxidant for the transformation of a wide range of organic compounds. Similar to S<sub>2</sub>O<sub>8</sub><sup>2-</sup>, undergo photolysis or thermolysis in aqueous solution, HSO<sub>5</sub><sup>-</sup> decomposes to generate reactive radicals such as SO<sub>4</sub><sup>•-</sup> and  $\cdot\text{OH}$  (Eq. (23)) [59,60];



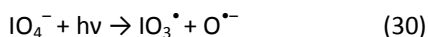
Bromate is an inorganic disinfection in the mineralization process with an oxidation potential of 1.4 V in acidic medium. Bromate under photolysis in aqueous solution decomposes to generate a number of various radical species,  $\text{BrO}_3^\bullet$ ,  $\text{O}^{\bullet-}$ ,  $\text{O}_2^-$ , etc (Eqs. (24)–(26)). Which the formation of these reactive species is responsible for the photooxidative activity of bromate [61,62].



The chlorate is an inorganic salt that functions as an oxidizing agent, particularly in the presence of strong acid, which is used for various medical, veterinary, and miscellaneous purposes. Chlorate anion is unstable in water and decomposes to form hypochlorite and oxygen and reacts readily with organic materials. The decomposition of  $\text{ClO}_3^-$  under UV irradiation showed in the following reactions (Eqs. (27)–(29)) [63];

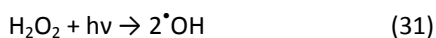


Periodate was described as an inorganic oxidant which can rapidly oxidize a wide range of organic compounds, that most of the organic compounds have the amine, imine or glycol group. Periodate under photolysis in aqueous solution decomposes to generate a number of highly reactive radicals and non-radical intermediates (Eq. (30)) [61–63];



The formation of various highly reactive radical species ( $\text{O}^{\bullet-}$ ,  $^{\bullet}\text{OH}$ ,  $\text{IO}_3^\bullet$  and  $\text{IO}_4^\bullet$ ) and non-radical intermediates ( $\text{O}_3$ ,  $\text{IO}_4^-$  and  $\text{IO}_3^-$ ) is responsible for the high activity of UV/ $\text{IO}_4^-$ .

Hydrogen peroxide is a strong oxidant with high active oxygen content, that the combined with UV light (UV/ $\text{H}_2\text{O}_2$ ) is a well-known advanced oxidation process for degradation of organic compounds. The decomposition of  $\text{H}_2\text{O}_2$  under UV irradiation showed in the following reaction (Eq. (31)) [67];



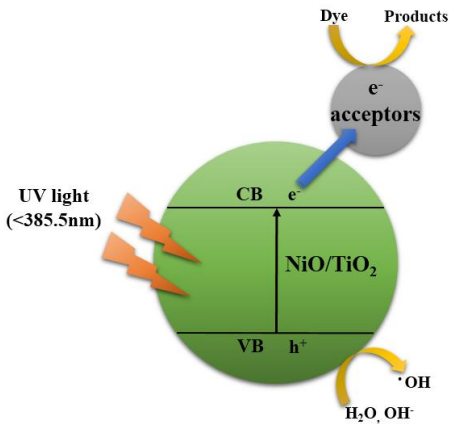


**FIGURE 4.17**  
Scavenging of photogenerated electrons by inorganic oxidants

The inhibitory effect of inorganic anions was explained by two factors; (i) The negative effect of inorganic anions is attributed to the competitive adsorption of anions and the target organic substance onto the surface of the catalyst, and resulting in blockage of the active sites on the catalyst surface hinder the photocatalytic degradation of organic substance by oxidative species. (ii) On the other hand, inorganic anions through scavenging of generated holes in the valence band and hydroxyl radicals causes a great impediment to the progress of the photocatalytic reaction (Figure 4.18).

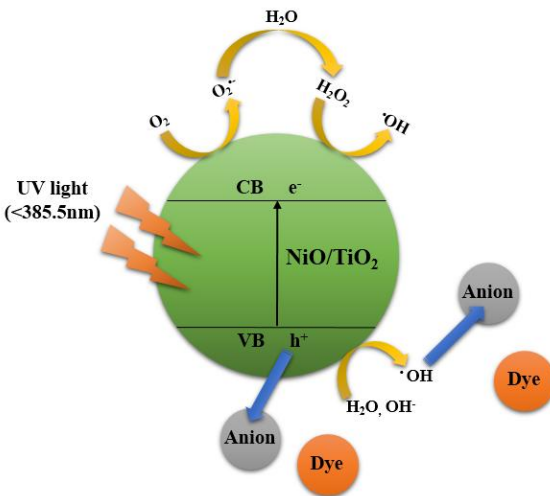


**FIGURE 4.18**  
Scavenging of positive holes and hydroxyl radicals by inorganic anions

## Conclusion

Titania is introduced as a promising photocatalyst to the destruction of organic pollutants. It is clearly revealed that the sol–gel synthesis variables affect the structural properties of titania and accordingly affect its photocatalytic activity. Doping with various metal species and coupling with other oxide semiconductors are possible solving routes to increase the lifetime of the photo-produced electron–hole pairs and improvement of the photocatalytic activity of titania. The negatively charged inorganic anions in wastewaters behaved like to  $h^+$  and  $\cdot OH$  scavengers and cause a negative effect on the photocatalytic processes. Whereas the dissolved metal ions in wastewaters and inorganic oxidants increase the electron–hole separation time, by accepting the conduction band electron and resulting in the improvement of the photocatalytic activity of titania.

## Acknowledgment

The authors would like to thank the University of Tehran for financial support of this work.

## References

1. Gibbons DC. The economic value of water. Routledge; 2013.
2. Levine AD, Asano T. Peer Reviewed: Recovering Sustainable Water from Wastewater. *Environmental Science & Technology* 2004;38(11) 201A–208A.
3. Barker DJ, Stuckey DC. (). A Review of Soluble Microbial Products (SMP) in Wastewater Treatment Systems. *Water research* 1999;33(14) 3063–3082.
4. Verma AK, Dash RR, Bhunia P. A Review on Chemical Coagulation/Flocculation Technologies for Removal of Colour from Textile Wastewaters. *Journal of Environmental Management* 2012;93(1) 154–168.
5. Preethi S, Sivasamy A, Sivanesan S, Ramamurthi V, Swaminathan G. Removal of Safranin Basic Dye from Aqueous Solutions by Adsorption onto Corncob Activated Carbon. *Industrial & Engineering Chemistry Research* 2006;45(22), 7627–7632.
6. Venkata Mohan S, Chandrasekhar Rao N, Krishna Prasad K, Karthikeyan J. Treatment of Simulated Reactive Yellow 22 (Azo) Dye Effluents Using Spirogyra Species. *Waste Management* 2002;22(6) 575–582.
7. Rai HS, Bhattacharyya MS, Singh J, Bansal TK, Vats P, Banerjee UC. Removal of Dyes from the Effluent of Textile and Dyestuff Manufacturing Industry: A Review of Emerging Techniques with Reference to Biological Treatment. *Critical Reviews in Environmental Science and Technology* 2005;35(3) 219–238.
8. Khataee AR, Fathinia M, Aber S, Zarei M. Optimization of Photocatalytic Treatment of Dye Solution on Supported  $TiO_2$  Nanoparticles by Central Composite Design: Intermediates Identification. *Journal of Hazardous Materials* 2010;181(1) 886–897.
9. Behnajady MA, Modirshahla N, Daneshvar N, Rabbani M. Photocatalytic Degradation of CI Acid Red 27 by Immobilized ZnO on Glass Plates in Continuous–Mode. *Journal of Hazardous Materials* 2007;140(1) 257–263.

10. Konstantinou IK, Albanis TA. TiO<sub>2</sub>-Assisted Photocatalytic Degradation of Azo Dyes in Aqueous Solution: Kinetic and Mechanistic Investigations: A Review. *Applied Catalysis B: Environmental* 2004;49(1) 1–14.
11. Gaya UI, Abdullah AH. Heterogeneous Photocatalytic Degradation of Organic Contaminants over Titanium Dioxide: A Review of Fundamentals, Progress and Problems. *Journal of Photochemistry and Photobiology C: Photochemistry Reviews* 2008;9(1) 1–12.
12. Rajeshwar K, Osugi ME, Chanmanee W, Chenthamarakshan CR, Zaroni MVB, Kajitvichyanukul P, Krishnan–Ayer R. Heterogeneous Photocatalytic Treatment of Organic Dyes in Air and Aqueous Media. *Journal of Photochemistry and Photobiology C: Photochemistry Reviews* 2008;9(4) 171–192.
13. Kwan CY, Chu W. Photodegradation of 2, 4–Dichlorophenoxyacetic Acid in Various Iron–Mediated Oxidation Systems. *Water research* 2003;37(18) 4405–4412.
14. Ibhaddon AO, Fitzpatrick P. Heterogeneous Photocatalysis: Recent Advances and Applications. *Catalysts* 2013;3(1) 189–218.
15. Behnajady MA, Modirshahla N, Daneshvar N, Rabbani M. Photocatalytic Degradation of C.I. Acid Red 27 by Immobilized ZnO on Glass Plates in Continuous–mode. *Journal Hazardous Material* 2007;140 257–263.
16. Chakrabarti S, Dutta BK. Photocatalytic Degradation of Model Textile Dyes in Wastewater Using ZnO as a Semiconductor Catalyst, *Journal Hazardous Material* 2004;112 269–278.
17. Behnajady MA, Eskandarloo H. Silver and Copper Co–Impregnated onto TiO<sub>2</sub>–P25 nanoparticles and its photocatalytic activity. *Chemical Engineering Journal* 2013;228 1207–1213.
18. Ni M, Leung MK, Leung DY, Sumathy K. A Review and Recent Developments in Photocatalytic Water–Splitting Using TiO<sub>2</sub> for Hydrogen Production. *Renewable and Sustainable Energy Reviews* 2007;11(3) 401–425.
19. Akpan UG, Hameed BH. Parameters Affecting the Photocatalytic Degradation of Dyes Using TiO<sub>2</sub>–Based Photocatalysts: A Review. *Journal of Hazardous Materials* 2009;170(2) 520–529.
20. Schwitzgebel J, Ekerdt JG, Gerischer H, Heller A. Role of the Oxygen Molecule and of the Photogenerated Electron in TiO<sub>2</sub>–Photocatalyzed Air Oxidation Reactions. *Journal of Physical Chemistry* 1995;99 5633–5638.
21. Xiong S, George S, Ji Z, Lin S, Yu H, Damoiseaux R, France B, Ng KW, Loo SCJ. Size of TiO<sub>2</sub> Nanoparticles Influences their Phototoxicity: An in Vitro Investigation. *Archives of Toxicology* 2013;87 99–109.
22. El–Kemary M, El–Shamy H, El–Mehasseb I. Photocatalytic Degradation of Ciprofloxacin Drug in Water Using ZnO Nanoparticles. *Journal of Luminescence* 2010;130 2327–2331.
23. Kowalska E, Rau S. Photoreactors for Wastewater Treatment: A Review. *Recent Patents on Engineering* 2010;4(3) 242–266.
24. Damodar RA, Jagannathan K, Swaminathan T. Decolourization of Reactive Dyes by thin Film Immobilized Surface Photoreactor Using Solar Irradiation. *Solar energy* 2007;81(1) 1–7.
25. Charles G, Roques–Carmes T, Becheikh N, Falk L, Commenge JM, Corbel S. Determination of Kinetic Constants of a Photocatalytic Reaction in Micro–Channel Reactors in the Presence of Mass–Transfer Limitation and Axial Dispersion. *Journal of Photochemistry and Photobiology A: Chemistry* 2011;223(2) 202–211.

26. Nishanthi ST, Henry Raja D, Subramanian E, Pathinettam Padiyan D. Remarkable Role of Annealing Time on Anatase Phase Titania Nanotubes and its Photoelectrochemical Response. *Electrochimica Acta* 2013;89 239–245.
27. Reyes–Coronado D, Rodriguez–Gattorno G, Espinosa–Pesqueira ME, Cab C, De Coss R, Oskam G. Phase–Pure TiO<sub>2</sub> Nanoparticles: Anatase, Brookite and Rutile. *Nanotechnology* 2008;19(14) 145605–14.
28. Moonosawmy KR, Katzke H, Es–Souni M, Dietze M, Es–Souni M. Mesoporous and Macroporous Brookite Thin Films Having a Large Thermal Stability Range. *Langmuir* 2012;28(16) 6706–6713.
29. Teh CM, Mohamed AR. Roles of Titanium Dioxide and Ion–Doped Titanium Dioxide on Photocatalytic Degradation of Organic Pollutants (Phenolic Compounds and Dyes) in Aqueous Solutions: A Review. *Journal of Alloys and Compounds* 2011;509(5) 1648–1660.
30. Chen X, Mao SS, Titanium Dioxide Nanomaterials: Synthesis, Properties, Modifications, and Applications. *Chemical Reviews* 2007;107 2891–2959.
31. Linsebigler AL, Lu G, Yates Jr JT. Photocatalysis on TiO<sub>2</sub> Surfaces: Principles, Mechanisms, and Selected Results. *Chemical reviews* 1995;95(3) 735–758.
32. Wang Z, Chen C, Wu F, Zou B, Zhao M, Wang J, Feng C, Photodegradation of Rhodamine B under Visible Light by Bimetal Codoped TiO<sub>2</sub> nanocrystals. *Journal of Hazardous Materials* 2009;164 615–620.
33. Hoffmann MR, Martin ST, Choi W, Bahnemann DW, Environmental Applications of Semiconductor Photocatalysis. *Chemical Reviews* 1995;95 69–96.
34. Henrist C, Dewalque J, Mathis F, Cloots R. Control of the Porosity of Anatase Thin Films Prepared by EISA: Influence of Thickness and Heat Treatment. *Microporous and Mesoporous Materials* (2009;117(1) 292–296.
35. Hernandez–Martinez AR, Estevez M, Vargas S, Rodriguez R. New Polyurethane–Anatase Titania Porous Hybrid Composite for the Degradation of Azo–Compounds Wastes. *Composites Part B: Engineering* 2013;44(1) 686–691.
36. Bessekhoud Y, Robert D, Weber JV. Synthesis of Photocatalytic TiO<sub>2</sub> Nanoparticles: Optimization of the Preparation Conditions. *Journal of Photochemistry and Photobiology A: Chemistry* 2003;157(1) 47–53.
37. Behnajady MA, Eskandarloo H, Modirshahla N, Shokri M. Sol–Gel Low-temperature Synthesis of Stable Anatase-Type TiO<sub>2</sub> Nanoparticles Under Different Conditions and its Photocatalytic Activity. *Photochemistry and Photobiology* 2011;87(5) 1002–1008.
38. Behnajady MA, Eskandarloo H, Modirshahla N, Shokri M. Investigation of the Effect of Sol–Gel Synthesis Variables on Structural and Photocatalytic Properties of TiO<sub>2</sub> Nanoparticles. *Desalination* 2011;278(1) 10–17.
39. Behnajady MA, Eskandarloo H, Preparation of TiO<sub>2</sub> Nanoparticles by the Sol–Gel Method under Different pH Conditions and Modeling of Photocatalytic Activity by Artificial Neural Network. *Research on Chemical Intermediates* 2015;41 2001–2017.
40. Xu T, Zhang L, Cheng H, Zhu Y. Significantly Enhanced Photocatalytic Performance of ZnO via Graphene Hybridization and the Mechanism Study. *Applied Catalysis B: Environmental* 2011;101(3) 382–387.
41. Zhang L, Zhu Y. A Review of Controllable Synthesis and Enhancement of Performances of Bismuth Tungstate Visible–Light–Driven Photocatalysts. *Catalysis Science & Technology* 2012;2(4) 694–706.

42. Song K, Zhou J, Bao J, Feng Y, Photocatalytic Activity of (Copper, Nitrogen)- Codoped Titanium Dioxide Nanoparticles. *Journal of the American Ceramic Society* 2008;91 1369–1371.
43. Ambrus Z, Balazs N, Alapi T, Wittmann G, Sipos P, Dombi A, Mogyorosi K, Synthesis, Structure and Photocatalytic Properties of Fe(III)-Doped TiO<sub>2</sub> Prepared from TiCl<sub>3</sub>. *Applied Catalysis B: Environmental* 2008;81 27–37.
44. Liqiang J, Honggang F, Baiqi W, Dejun W, Baifu X, Shudan L, Jiazhong S, Effects of Sn Dopant on the Photoinduced Charge Property and Photocatalytic Activity of TiO<sub>2</sub> Nanoparticles. *Applied Catalysis B: Environmental* 2006;62 282–291.
45. Pelaez M, Nolan NT, Pillai SC, Seery MK, Falaras P, Kontos AG, Dunlop PSM, Hamilton JWJ, Byrne JA, O'Shea K, Entezari MH, Dionysiou DD. A Review on the Visible Light Active Titanium Dioxide Photocatalysts for Environmental Applications. *Applied Catalysis B: Environmental* 2012;125 331–349.
46. Castro AL, Nunes MR, Carvalho MD, Ferreira LP, Jumas JC, Costa FM, Florêncio MH. Doped Titanium Dioxide Nanocrystalline Powders with High Photocatalytic Activity. *Journal of Solid State Chemistry* 2009;182(7) 1838–1845.
47. Behnajady MA, Eskandarloo H. Characterization and Photocatalytic Activity of Ag–Cu/TiO<sub>2</sub> Nanoparticles Prepared by Sol–Gel Method. *Journal of Nanoscience and Nanotechnology* 2013;13(1) 548–553.
48. Kumar SG, Devi LG. Review on Modified TiO<sub>2</sub> Photocatalysis under UV/Visible Light: Selected Results and Related Mechanisms on Interfacial Charge Carrier Transfer Dynamics. *The Journal of Physical Chemistry A* 2011;115(46) 13211–13241.
49. Liu L, Ji Z, Zou W, Gu X, Deng Y, Gao F, Tang C, Dong L. In Situ Loading Transition Metal Oxide Clusters on TiO<sub>2</sub> Nanosheets As Co-catalysts for Exceptional High Photoactivity. *ACS Catalysis* 2013;3(9) 2052–2061.
50. Eskandarloo H, Badiiei A, Behnajady MA. TiO<sub>2</sub>/CeO<sub>2</sub> Hybrid Photocatalyst with Enhanced Photocatalytic Activity: Optimization of Synthesis Variables. *Industrial & Engineering Chemistry Research*. 2014;53 7847–7855.
51. Eskandarloo H, Badiiei A, Behnajady MA. Study of the Effect of Additives on the Photocatalytic Degradation of a Triphenylmethane Dye in the Presence of Immobilized TiO<sub>2</sub>/NiO Nanoparticles: Artificial Neural Network Modeling. *Industrial & Engineering Chemistry Research*. 2014;53 6881–6895.
52. Ravichandran L, Selvam K, Swaminathan M. Effect of Oxidants and Metal ions on Photodefluorination of Pentafluorobenzoic Acid with ZnO. *Separation and Purification Technology* 2007;56 192–198.
53. Selvam K, Muruganandham M, Muthuvel I, Swaminathan M. The Influence of Inorganic Oxidants and Metal Ions on Semiconductor Sensitized Photodegradation of 4-Fluorophenol. *Chemical Engineering Journal* 2007;128 51–57.
54. Chen C, Li X, Ma W, Zhao J, Hidaka H, Serpone N. Effect of Transition Metal Ions on the TiO<sub>2</sub>-Assisted Photodegradation of Dyes under Visible Irradiation: A Probe for the Interfacial Electron Transfer Process and Reaction Mechanism. *The Journal of Physical Chemistry B* 2002;106 318–324.
55. Muruganandham M, Swaminathan M. Photocatalytic Decolourisation and Degradation of Reactive Orange 4 by TiO<sub>2</sub>-UV Process. *Dyes and Pigments* 2006;68 133–142.
56. Eskandarloo H, Badiiei A, Behnajady MA. Optimization of UV/Inorganic Oxidants System Efficiency for Photooxidative Removal of an Azo Textile Dye. *Desalination and Water Treatment* doi: 10.1080/19443994.2014.912965.

57. Lau TK, Chu W, Graham NJD. The Aqueous Degradation of Butylated Hydroxyanisole by UV/S<sub>2</sub>O<sub>8</sub><sup>2-</sup>: Study of Reaction Mechanisms via Dimerization and Mineralization. *Environmental Science & Technology* 2007;41 613–619.
58. Khataee AR, Mirzajani O. UV/Peroxydisulfate Oxidation of C. I. Basic Blue 3: Modeling of Key Factors by Artificial Neural Network. *Desalination* 2010;251 64–69.
59. Yang Y, Wang P, Yang X, Shan L, Zhang WY, Shao XT, Niu R. Degradation Efficiencies of Azo Dye Acid Orange 7 by the Interaction of Heat, UV and Anions with Common Oxidants: Persulfate, Peroxymonosulfate and Hydrogen Peroxide. *Journal Hazardous Material* 2010;179 552–558.
60. Hayon E, Treinin A, Wilf J. Electronic Spectra, Photochemistry, and Autoxidation Mechanism of the Sulfite–Bisulfite–Pyrosulfite Systems. SO<sub>2</sub><sup>-</sup>, SO<sub>3</sub><sup>-</sup>, SO<sub>4</sub><sup>-</sup>, and SO<sub>5</sub><sup>-</sup> Radicals. *Journal of the American Chemical Society* 1972;94 47–57.
61. Zuo Z, Katsumura Y. Formation of Hydrated Electron and BrO<sub>3</sub> Radical from Laser Photolysis of BrO<sub>3</sub><sup>-</sup> Aqueous Solution. *Journal of the Chemical Society, Faraday Transactions* 1998;94 3577–3580.
62. Sahoo MK, Marbaniang M, Sinha B, Naik DB, Sharan RN. UVC Induced TOC Removal Studies of Ponceau S in the Presence of Oxidants: Evaluation of Electrical Energy Efficiency and Assessment of Biototoxicity of the Treated Solutions by Escherichia Coli Colony Forming Unit Assay. *Chemical Engineering Journal* 2012;213 142–149.
63. Stauber JL. Toxicity of Chlorate to Marine Microalgae. *Aquatic Toxicology* 1998;41 213–227.
64. Wang Y, Hong CS. Effect of Hydrogen Peroxide, Periodate and Persulfate on Photocatalysis of 2-Chlorobiphenyl in Aqueous TiO<sub>2</sub> Suspensions. *Water Research* 1999;33 2031–2036.
65. Lee C, Yoon J. Application of Photoactivated Periodate to the Decolorization of Reactive Dye: Reaction Parameters and Mechanism, *Journal of Photochemistry and Photobiology A: Chemistry* 2004;165 35–41.
66. Sadik WA. Effect of Inorganic Oxidants in Photodecolourization of an Azo Dye. *Journal of Photochemistry and Photobiology A: Chemistry* 2007;191 132–137.
67. Saien J, Soleymani AR, Sun JH. Parametric Optimization of Individual and Hybridized AOPs of Fe<sup>2+</sup>/H<sub>2</sub>O<sub>2</sub> and UV/S<sub>2</sub>O<sub>8</sub><sup>2-</sup> for Rapid Dye Destruction in Aqueous Media. *Desalination* 2011;279 298–305.